Uniparabolic mirror grading for vertical cavity surface emitting lasers

K. L. Lear[a] and R. P. Schneider, Jr.[b]
Sandia National Laboratories, Photonics Research Department 1312, MS 0603, P.O. Box 5800, Albuquerque, New Mexico 87185-0603

(Received 31 July 1995; accepted for publication 9 November 1995)

We report details of mirror grading profiles for high efficiency vertical cavity surface emitting lasers. The mirrors provide low vertical resistance in conjunction with improvements in optical reflectivity, thermal conductivity, and lateral electrical conductivity in comparison to earlier grading profiles. The enhancement of these properties is verified by a comparison of thermal resistance and total electrical resistance for lasers of varying size. © *1996 American Institute of Physics.* [S0003-6951(96)00704-9]

Research during the past few years has made substantial progress in reducing the operating voltages of vertical-cavity surface-emitting lasers (VCSELs).[1–3] Sophisticated heterojunction grading and doping methods have reduced the high voltage drops of early multilayer, semiconducting distributed Bragg reflectors (mirrors). These methods include step grading combined with delta doping[4,5] and modulation doped parabolic grades.[6,7] Previous work at Sandia[8] used cyclical effusion cell temperature variation to produce mirrors with piecewise linearly graded alloy composition by molecular beam epitaxy (MBE). These grading approaches were successful at reducing vertical mirror resistance but often at the expense of other important properties.

In addition to conducting current vertically, semiconducting mirror stacks should also have good thermal conductivity, maximum optical reflectivity per period, and for top emitting devices with annular contacts, high lateral electrical conductivity. In general, it is desirable to minimize the alloy content of mirrors in order to achieve these goals. Alloy scattering reduces both the electronic mobilities and thermal conductivity of alloys with respect to the constituent compounds.[9] Since refractive indices vary monotonically with alloy composition, index changes and thus reflectivity are reduced in mirrors with narrowed composition ranges. Excessively wide graded regions can also reduce reflectivity. Thus, alloy content and grading must be chosen to balance the requirements for low vertical resistance with the other properties. Specifically, alloy grading should be concentrated in large band-gap regions prone to depletion where it has the greatest benefit.

These considerations have led to a redesign of our earlier piecewise linearly graded mirrors. The old and new mirror designs are shown in Fig. 1. Previously, the mirror composition varied between $Al_{0.1}Ga_{0.9}As$ and $Al_{0.9}Ga_{0.1}As$ within a 56 nm graded region. Continuous grading to binary GaAs and AlAs compositions was not possible by MBE without shuttering due to limitations on cell temperature excursions. In contrast, the new grading profile goes from GaAs to $Al_{0.96}Ga_{0.04}As$ within a graded region of 28 nm. These structures were grown by metalorganic vapor phase epitaxy (MOVPE) which also cannot reliably grade continuously between binary compositions due to limited dynamic ranges for stable mass flow controller operation. In order to reach GaAs, the Al source is switched to change abruptly between $Al_{0.1}Ga_{0.9}As$ and GaAs. A similar structure could be grown by MBE with appropriate control software.

The extent of non-Ohmic transport limitations can be inferred from the equilibrium valence band profiles for these structures as shown by the dotted lines in Fig. 1. Upward and downward pointing potential cusps, respectively corresponding to narrow depletion and accumulation regions, form at the slope discontinuities present in the piecewise linearly graded profile. Only the upward cusps in depletion regions act as significant barriers to hole transport. The downward cusps occur at accumulation layers which do not significantly inhibit conductivity relative to the flatband regions. Trapping of carriers vertically transiting the accumulation regions in downward cusps is negligible due to near-degenerate doping.

The new grading profile results in an elimination of only those band edge features that most substantially hinder vertical current flow. The computed equilibrium valence band profile shows no depleted upward cusps to inhibit carrier motion. A deep accumulation region that enhances lateral conduction forms at the abrupt $GaAs/Al_{0.1}Ga_{0.9}As$ heterojunction. However, the band edge discontinuity must be limited to a few thermal voltages (kT) to prevent a depletion region from forming on the AlGaAs side. Only a single, negative curvature parabolic segment is used to smooth the transition to the large band-gap material. We have termed this grading profile ''uniparabolic'' to distinguish it from one with two concatenated parabolic segments (''biparabolic'') of opposite curvature as used by others.[6,7] The use of a uniparabolic profile substantially reduces the graded region relative to biparabolic profiles of equal curvature, improving thermal, optical, and lateral electrical properties. As in the case of modulation doped biparabolic grading, doping levels must be changed commensurately with the curvature of parabolic regions.[6,7] The concave downward uniparabolic segments require an increased acceptor concentration in the *p*-type mirrors. This space charge is balanced by the holes in the accumulation layer.

[a]Electronic mail: kllear@sandia.gov
[b]Present address: Hewlett-Packard Laboratory, MS 26M10, 3500 Deer Creek Road, Palo Alto, CA 94304

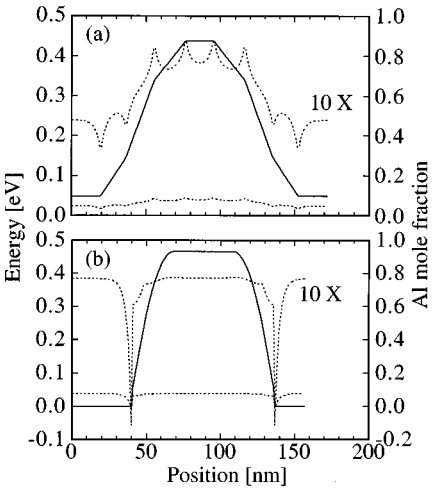

FIG. 1. The zero-field (solid) and equilibrium (dotted) valence band minimum hole energy profiles referenced to GaAs and the Fermi energy, respectively. (The plots are inverted from the usual convention so that hole energy increases upward). The solid curves can also be read against the right axis as the approximate aluminum mole fraction. Profiles are shown for (a) three segment per interface piecewise linear grading and (b) uniparabolic grading.

Measurements on *p*-type mirror stacks and full VCSEL structures confirm that the uniparabolic grading approach simultaneously reduces vertical electrical resistance, lateral electrical resistance, and thermal resistance in comparison to earlier three-segment piecewise linear grading. Note that the growth method changed from MBE to MOVPE and acceptor species changed from beryllium to carbon in conjunction with the change from piecewise linear to uniparabolic grading profiles. The acceptor density was adjusted to produce nominally uniform hole concentrations except in the parabolic regions. Hall measurements on bulk samples of various alloy content confirmed the activated hole concentrations. In particular, the Be flux was adjusted to compensate for the reduced doping efficiency in high Al content regions.[8,10] Calculated and measured properties for the two mirror designs are summarized in Table I. These numbers indicate substantial optical, thermal, and electrical improvements.

TABLE I. Properties of two mirror grading schemes illustrated in Fig. 1.

Grading profile	Uniparabolic [Fig. 1(b)]	2 segment piecewise linear [Fig. 1(a)]
Computed maximum energy ($E_V - E_F$) (meV)	39	43
Acceptor species and hole concentration ($\times 10^{18}$ cm^{-3})	C, 2.6 in parabolic grades, 2.0 elsewhere	Be, 2.0
Meas. vertical resistance ($\times 10^{-6}$ Ω cm^2/period)	0.96	1.9
Calc. lateral resistance (kΩ-period/□)	2.10	2.96
Calc. field reflection coeff. per interface	0.0787	0.0572
Calc. lateral thermal conductivity (W/cm K)	0.357	0.168
Calc. vertical thermal conductivity (W/cm K)	0.273	0.155

The vertical mirror resistance for 10 period, carbon-doped mirror stacks with uniparabolic grading was determined from 4-wire voltage versus current measurements of 30 μm diameter reactive ion etched mesas. The samples were grown by MOVPE on heavily doped substrates. The mirrors exhibited linear current–voltage relationships indicating the absence of significant non-Ohmic transport barriers. Contact resistance, as determined from test structures on the sample, and substrate spreading resistance were subtracted from the total resistance to analyze the contribution from the mirrors alone. The resulting areal resistivities were 2.7×10^{-6} and 0.96×10^{-6} Ω cm^2/period for base carbon doping levels of 1×10^{18} and 2×10^{18} cm^{-3}, respectively.

As mentioned in the introduction, low lateral resistances are crucial for top emitting devices with annular contacts.[11] Therefore, such devices serve as a convenient means for evaluating the lateral resistance of mirrors. The total device resistance of top-emitting, proton-implanted VCSELs based on the two mirror designs of Fig. 1 is presented as a function of device size in Fig. 2. In addition to the different mirrors, the uniparabolic mirror lasers were capped with an additional, heavily doped, half-wavelength contact and current spreading layer with a calculated sheet resistance of 168 Ω/□. This cap in parallel with a 20 period uniparabolic mirror sheet resistance of 105 Ω/□ yields a combined calculated sheet resistance of 65 Ω/□ for the MOVPE devices. The calculated sheet resistance for 22 period *p*-mirror MBE devices without the extra half-wavelength cap is 135 Ω/□, twice that of the MOVPE devices. The devices had commensurate implant defined gain regions and contact apertures and were fabricated as previously described.[1,11] The 4-wire resistance was measured between threshold and peak power bias points. The lasers with uniparabolic, carbon doped mirrors show a dramatic decrease in resistance in comparison to their piecewise, linearly graded counterparts.

The resistance dependence on size can be further analyzed by fitting it to the empirical formula[11], $R = R_L/r + R_v/\pi r^2$. The first term varies inversely with the device perimeter to account for contact, lateral, and constriction resistance contributions. The second term varies inversely with

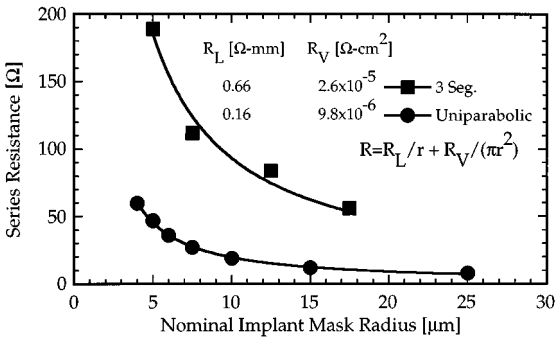

FIG. 2. The series resistance as a function of active region radius for proton implant defined VCSELs incorporating (circles) MOVPE mirrors with uniparabolic grading and (squares) MBE mirrors with three linear segments per interface grading. The curves indicate fits of the equation to both sets of data with the fitting parameters indicated.

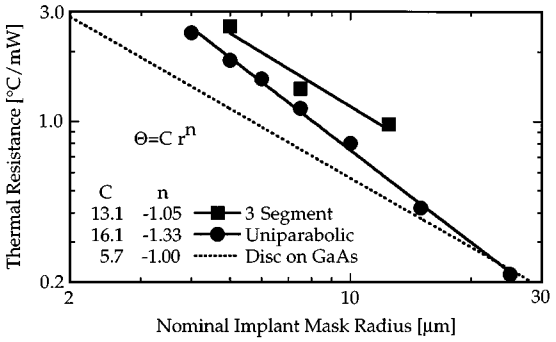

FIG. 3. The thermal resistance as a function of active region radius for proton implant defined VCSELs incorporating (circles) MOVPE mirrors with uniparabolic grading and (squares) MBE mirrors with three linear segments per interface grading. The solid curves indicate power law fits in the radius with the constants shown. The dotted curve is the theoretical resistance of a uniform temperature disc on the surface of a semi-infinite GaAs region.

area to reflect voltage drops associated with uniform vertical current flow through the mirror. Fits and fitting parameters are shown in the figure for the two sets of data. In both cases the first, lateral, resistance term dominates for device radii larger than ~ 1 μm. This emphasizes the importance of reducing lateral resistance in top-emitting VCSELs. The lateral resistance fitting parameter R_L, is four times lower for the uniparabolic mirror lasers as compared to the piecewise linear graded mirror lasers. This factor is greater than the ratio of calculated sheet resistances. The enhancement may be due to the nonlinear dependence of contact resistance on carrier concentration, especially in partially compensated, implanted regions.

Scaling data as a function of device size is also insightful for evaluating the thermal resistance of the mirrors. A logarithmic plot of thermal resistance against laser radius is shown in Fig. 3. The lasers' temperature change was measured from the spectral shift of laser modes using a coefficient of 0.07 nm/K. This value was determined from observation of spectral shifts with ambient (stage) temperature. Again, the reduced alloy content of the uniparabolic mirrors yielded the expected reduction in thermal resistance compared to the piecewise linearly graded mirrors. (The thermal conductivities were calculated according to the laminar model based on bulk thermal conductivities of alloys[9] and thus neglect effects of doping or interfacial scattering.[12]) The coefficient and exponent of a sample fit to a power curve for the two data sets are presented in the figure. The ideal thermal constriction resistance for a uniform temperature disc on an infinitely thick GaAs substrate is also shown. For devices much larger than the ~ 5 μm mirror thickness, the heat flow is mostly vertical through the bottom mirror. In this regime, the difference in thermal resistances approximately agrees with the value expected from the difference in perpendicular thermal conductivity of the mirrors. For large devices, the actual uniparabolic thermal resistance can cross the idealized value due to finite substrate thickness and nonuniform heat distribution. Ideally, small devices should emphasize the difference in mirror thermal resistance. The convergence of the curve fits with decreasing device size suggests that lateral heatsinking through the contact metallization may become important.

Reduced resistance and thus reduced heat generation combines with better thermal conductivity to impact device performance through substantial reductions in operating temperature. This has increased the maximum single-mode and multimode power of proton-implanted, uniparabolic mirror VCSELs in wafer form to 4.4 and 23 mW, respectively.[1] Power conversion efficiencies are enhanced by both the lower voltage drops and decreased temperature. Recently, uniparabolic mirrors have been combined with AlGaAs oxidation confinement to produce threshold voltages as low as 1.33 V,[2] and power conversion efficiencies up to 50%.[13]

In conclusion, a new type of grading, termed uniparabolic, balances the pertinent properties of VCSEL mirrors including vertical and lateral electrical resistance, thermal resistance, and optical reflectivity. The grading profile is based on the philosophy of using a minimal alloy content to grade only those regions necessary to achieving Ohmic vertical mirror transport. Specifically, depletion regions are eliminated with a modulation doped parabolic grade, but accumulation regions are retained and enhanced. Experimental measurements of mirror current–voltage characteristics, total device resistance, and laser operating temperature have confirmed improvements to electrical and thermal resistances.

The authors thank K. Choquette for useful discussion and J. Figiel, S. Kilcoyne, and J. Nevers for technical assistance. This work was supported by the United States Department of Energy under Contract No. DE-AC04-94AL85000.

[1] K. L. Lear, R. P. Schneider, Jr., K. D. Choquette, S. P. Kilcoyne, J. J. Figiel, and J. C. Zolper, Photon. Technol. Lett. **6**, 1053 (1994).
[2] K. D. Choquette, R. P. Schneider, Jr., K. L. Lear, and K. M. Geib, Electron. Lett. **30**, 2043 (1994).
[3] R. A. Morgan, M. K. Hibbs-Brenner, J. A. Lehman, E. L. Kalweit, R. A. Walterson, T. M. Marta, and T. Akinwande, Appl. Phys. Lett. **66**, 1157 (1995).
[4] K. Kojima, R. A. Morgan, T. Mullally, G. D. Guth, M. W. Focht, R. E. Leibenguth, and M. T. Asom, Electron. Lett. **29**, 1771 (1993).
[5] G. Reiner, E. Zeeb, B. Möller, M. Ries, and K. J. Ebeling, Photonics Technol. Lett. **7**, 730 (1995).
[6] E. F. Schubert, L. W. Tu, G. J. Zydzik, R. F. Kopf, A. Benvenuti, and M. R. Pinto, Appl. Phys. Lett. **60**, 466 (1992).
[7] M. G. Peters, B. J. Thibeault, D. B. Young, J. W. Scott, F. H. Peters, A. C. Gossard, and L. A. Coldren, Appl. Phys. Lett. **63**, 3411 (1993).
[8] S. A. Chalmers, K. L. Lear, and K. P. Killeen, Appl. Phys. Lett. **62**, 1585 (1993).
[9] S. Adachi, J. Appl. Phys. **58**, R1 (1985); see also S. Adachi and N. S. Takahashi, in *Properties of Aluminum Gallium Arsenide, EMIS Datareviews Series* (INSPEC, IEE, London, 1993), Vol. 7.
[10] R. F. Kopf, E. F. Schubert, S. W. Downey, and A. B. Emerson, Appl. Phys. Lett. **61**, 1820 (1992).
[11] K. L. Lear, S. P. Kilcoyne, and S. A. Chalmers, Photon. Tech. Lett. **6**, 778 (1994).
[12] G. Chen, C. L. Tien, X. Wu, and J. S. Smith, ASME J. Heat Transfer **116**, 325 (1994).
[13] K. L. Lear, K. D. Choquette, R. P. Schneider, Jr., S. P. Kilcoyne, and K. M. Geib, Electron. Lett. **31**, 208 (1995).